

HEAVILY OBSCURED AGN IN HIGH REDSHIFT LUMINOUS INFRARED GALAXIES

EZEQUIEL TREISTER^{1,2}, C. MEGAN URRY^{3,4,5}, KEVIN SCHAWINSKI^{2,4,5}, CAROLIN N. CARDAMONE^{3,4}, DAVID B. SANDERS¹

ApJ Letters, in press

ABSTRACT

We take advantage of the rich multi-wavelength data available in the Chandra Deep Field South (CDF-S), including the 4 Msec Chandra observations (the deepest X-ray data to date), in order to search for heavily-obscured low-luminosity AGN among infrared-luminous galaxies. In particular, we obtained a stacked rest-frame X-ray spectrum for samples of galaxies binned in terms of their IR luminosity or stellar mass. We detect a significant signal at $E \sim 1$ to 8 keV, which we interpret as originating from a combination of emission associated with star-formation processes at low energies combined with a heavily-obscured AGN at $E > 5$ keV. We further find that the relative strength of this AGN signal decays with decreasing IR luminosity, indicating a higher AGN fraction for more luminous IR sources. Together, these results strongly suggest the presence of a large number of obscured AGN in IR-luminous galaxies. Using samples binned in terms of stellar mass in the host galaxy, we find a significant excess at $E = 6-7$ keV for sources binned with $M > 10^{11} M_{\odot}$, consistent with a large obscured AGN population in high mass galaxies. In contrast, no strong evidence of AGN activity was found for less-massive galaxies. The integrated intensity at high energies indicates that a significant fraction of the total black hole growth, $\sim 22\%$, occurs in heavily-obscured systems that are not individually detected in even the deepest X-ray observations. There are also indications that the number of low-luminosity, heavily-obscured AGN does not evolve significantly with redshift, in contrast to the strong evolution seen in higher luminosity sources.

Subject headings: galaxies: active — galaxies: Seyfert — X-rays: galaxies — X-rays: diffuse background

1. INTRODUCTION

Most of the accretion onto the supermassive black hole (SMBH) found in the center of most massive galaxies is heavily obscured by the surrounding dust and gas (e.g., Fabian & Iwasawa 1999). In the local Universe, $\sim 75\%$ of the Seyfert 2 galaxies are heavily-obscured ($N_H > 10^{23} \text{ cm}^{-2}$; Risaliti et al. 1999). Many of these, if at $z \gtrsim 1$, where most of the black hole growth occurs, would not be identified in X-rays even in very deep (> 1 Msec) Chandra or XMM/Newton exposures (Treister et al. 2004). Locating and quantifying this heavily obscured SMBH growth, in particular at high redshifts, is currently one of the fundamental problems in astrophysics.

Because the energy absorbed at optical to X-ray wavelengths is later re-emitted in the mid-IR, it is expected that all Active Galactic Nuclei (AGN), even the most obscured ones, should be very bright mid-IR sources (e.g., Martínez-Sansigre et al. 2006). Hence, it is not surprising that a large number of heavily obscured — even Compton-thick ($N_H > 10^{24} \text{ cm}^{-2}$) — AGN have been found amongst the Luminous and Ultra-luminous Infrared Galaxies ((U)LIRGs; $L_{IR} > 10^{11}$ and $> 10^{12} L_{\odot}$ respectively), both locally (Iwasawa et al. 2009) and at high redshift (Bauer et al. 2010). Deep X-ray ob-

servations performed using the XMM-Newton (e.g., Braito et al. 2003, 2004), Chandra (Teng et al. 2005) and Suzaku (Teng et al. 2009) observatories have shown that most ULIRGs are intrinsically faint X-ray sources, most likely due to the effects of obscuration, while their X-ray spectra show combined signatures of starburst and AGN activity. The key features observed in the X-ray spectra of ULIRGs are a soft thermal component, typically associated with star formation, a heavily-obscured ($N_H \sim 10^{24} \text{ cm}^{-2}$) power-law associated with the AGN direct emission, and a prominent emission line at ~ 6.4 keV, identified with fluorescence emission from iron in the K_{α} ionization level, originating either in the accretion disk or in the surrounding material (Matt et al. 1991).

The presence of heavily-obscured AGN among the most extreme ULIRGs at $z \simeq 1-2$ has recently been established from deep Spitzer observations (Daddi et al. 2007; Fiore et al. 2008; Treister et al. 2009b). Most of these sources have very high, quasar-like, intrinsic luminosities, and hence most likely do not constitute the bulk of the heavily-obscured AGN population (Treister et al. 2010). Establishing the fraction of (U)LIRGs that host a lower luminosity AGN is a more challenging task. Recent works based on X-ray stacking (Fiore et al. 2009) and using 70- μm selected sources (Kartaltepe et al. 2010) report a steep decrease in the fraction of AGN with decreasing IR luminosity, going from $\sim 100\%$ at $L_{IR} = 10^{13} L_{\odot}$ to $< 10\%$ at $L_{IR} = 10^{10} L_{\odot}$. In the local Universe, Schawinski et al. (2010a) found that the incidence of low-luminosity, Seyfert-like, AGN as a function of stellar mass is more complicated, and is influenced by other parameters. For example, the dependence of AGN fraction on stellar mass can be opposite if galaxy morphology is considered (increases with decreas-

¹ Institute for Astronomy, 2680 Woodlawn Drive, University of Hawaii, Honolulu, HI 96822; treister@ifa.hawaii.edu

² Chandra/Einstein Fellow

³ Department of Astronomy, Yale University, PO Box 208101, New Haven, CT 06520.

⁴ Yale Center for Astronomy and Astrophysics, P.O. Box 208121, New Haven, CT 06520.

⁵ Department of Physics, Yale University, P.O. Box 208121, New Haven, CT 06520.

ing mass in the early-type galaxy population).

In this work, we estimate the fraction of heavily-obscured AGN in mid-IR-luminous and massive galaxies at high redshift, few of which are individually detected in X-rays. The main goal is to constrain the amount of obscured SMBH accretion happening in distant galaxies. This can be done thanks to the very deep X-ray observations available in the Chandra Deep Fields and the very low and stable Chandra background, which allows for the efficient stacking of individually undetected sources. Throughout this letter, we assume a Λ CDM cosmology with $h_0=0.7$, $\Omega_m=0.27$ and $\Omega_\Lambda=0.73$, in agreement with the most recent cosmological observations (Hinshaw et al. 2009).

2. ANALYSIS AND RESULTS

By stacking individually-undetected sources selected at longer wavelengths, it is possible to detect very faint X-ray emitters using Chandra observations. For example, this technique was used successfully by Brandt et al. (2001) in the Chandra Deep Field North (CDF-N) to measure the average X-ray emission from a sample of Lyman break galaxies at $z \simeq 2-4$ and by Rubin et al. (2004) to detect X-rays from red galaxies at $z \sim 2$. More recently, samples of heavily-obscured AGN candidates selected based on their mid-IR properties have been studied in X-rays via Chandra stacking (e.g., Daddi et al. 2007; Fiore et al. 2008; Treister et al. 2009b).

The 4 Msec Chandra observations of the Chandra Deep Field South (CDF-S), are currently the deepest view of the X-ray sky. In addition, the CDF-S has been observed extensively at many wavelengths. The multiwavelength data available on the (E)CDF-S were presented by Treister et al. (2009b). Very relevant for this work are the deep Spitzer observations available in this field, using both the Infrared Array Camera (IRAC) and the Multiband Imaging Photometer for Spitzer (MIPS), from 3.6 to 24 μm . Also critical is the availability of good quality photometric redshifts ($\Delta z/(1+z)=0.008$ for $R < 25.2$) obtained thanks to deep observations in 18 medium-band optical filters performed using Subaru/Suprime-Cam (Cardamone et al. 2010a).

We generated our sample starting with the 4959 Spitzer/MIPS 24 μm sources in the region covered by the Chandra observations that have photometric redshift $z > 0.5$, and hence rest-frame $E > 4$ keV emission falling in the high-sensitivity Chandra range. In addition, sources individually detected in X-rays and reported in the catalogs of Luo et al. (2008), Lehmer et al. (2005) or Virani et al. (2006) were removed from our sample, as these sources will otherwise dominate the stacked spectrum. We then inspected the remaining sources to eliminate individual detections in the 4 Msec data not present in the 2 Msec catalog of Luo et al. (2008). We further excluded 28 sources that meet the selection criteria of Fiore et al. (2008) for heavily obscured AGN, $f_{24}/f_R > 1000$ and $R-K > 4.5$ (Vega), because we expect these sources to contain an intrinsically luminous AGN (quasar), while the aim of this work is to find additional hidden accretion in less luminous objects. The median redshift of the sources in our final sample is 1.32 (average $z=1.5$) with a standard deviation of 0.77.

In order to perform X-ray stacking in the rest-frame, we started with the regenerated level 2 merged event

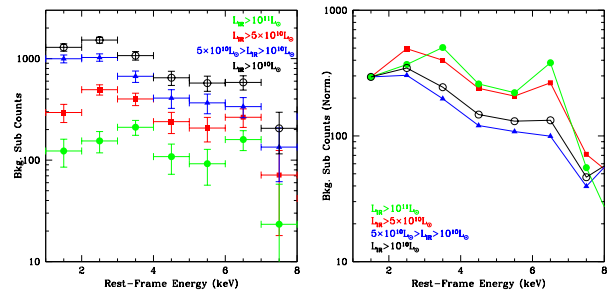


FIG. 1.— *Left panel:* Stacked background-subtracted Chandra counts as a function of rest-frame energy from 1 to 8 keV. Samples were selected based on their IR luminosity in the following overlapping bins: $L_{IR} > 10^{11} L_\odot$ (filled circles), $L_{IR} > 5 \times 10^{10} L_\odot$ (squares), $5 \times 10^{10} L_\odot > L_{IR} > 10^{10} L_\odot$ (triangles) and $L_{IR} > 10^{10} L_\odot$ (open circles). *Right panel:* same as left panel but normalized at 1 keV in order to highlight the differences in spectral shape among the different samples. The largest differences are at $E \gtrsim 5$ keV, where there is a clear trend in the relative intensity as a function of IR luminosity, suggesting a larger fraction of AGN in the most luminous IR sources.

files created by the Chandra X-ray Center⁶. For each source, we extracted all events in a circle of 30'' radius centered in the optical position. The energy of each event was then converted to the rest frame using the photometric redshift of the source. Using standard CIAO (Fruscione et al. 2006) tools we then generated seven X-ray images for each source covering the energy range from 1-8 keV in the rest-frame with a fixed width of 1 keV. Images for individual sources were then co-added to measure the stacked signal. Total counts were measured in a fixed 5'' aperture, while the background was estimated by randomly placing apertures with same the area, 5'' to 30'' away from the center.

Several groups have found (e.g. Kartaltepe et al. 2010 and references therein) that the fraction of galaxies containing an AGN is a strong function of their IR luminosity. Hence, it is a natural choice to divide our sample in terms of total IR luminosity. The infrared luminosity was estimated from the observed 24 μm luminosity assuming the relation found by Takeuchi et al. (2005): $\log(L_{IR})=1.02+0.972 \log(L_{12 \mu\text{m}})$. We further assumed that the k correction between observed-frame 24 μm and rest-frame 12 μm luminosity for these sources is negligible, as shown by Treister et al. (2009b). We then separated our sample in 4 overlapping bins: $L_{IR} > 10^{11} L_\odot$, $L_{IR} > 5 \times 10^{10} L_\odot$, $5 \times 10^{10} L_\odot > L_{IR} > 10^{10} L_\odot$ and $L_{IR} > 10^{10} L_\odot$ and stacked them independently. The number of sources in each sample is 670, 1545, 2342 and 3887 respectively.

In Fig. 1 we present the stacked spectra as a function of rest-frame energy, both in total counts and normalized at 1 keV to highlight the difference in spectral shape among the different samples. At $E \gtrsim 5$ keV, the spectra begin to diverge, where we expect the AGN emission to dominate even for heavily-obscured sources. There is a clear trend, with more high energy X-ray emission with increasing IR luminosity.

3. DISCUSSION

The spectra shown in Fig. 1 cannot be directly interpreted, as the detector-plus-telescope response information is lost after the conversion to rest-frame energy and stacking. Hence, we perform simulations assuming different intrinsic X-ray spectra in order to constrain the nature of the sources dominating the co-added signal. We use the XSPEC code (Arnaud 1996) to convolve several intrinsic input spectra with the latest response functions⁷ for the Chandra ACIS-I camera used in the CDF-S observations. We then compare these simulated spectra with the observations in our sample of IR-selected sources.

The low energy spectrum of (U)LIRGs is dominated by a combination of a thermal plasma component with temperatures $kT \simeq 0.7$ keV, particularly important at $E < 3$ keV, and the emission from high-mass X-ray binaries (HMXBs) at $1 < E$ (keV) < 10 (e.g., Persic & Rephaeli 2002). For each source, we generated a simulated spectrum using a combination of these two components, taking into account the luminosity and redshift of the source. For the HMXB population we assumed a power-law given by $\Gamma = 1.2$ and cutoff energy $E_c = 20$ keV, consistent with recent observations (e.g., Lutovinov et al. 2005). This component was normalized assuming the relation between IR and X-ray luminosity in starburst galaxies found by Ranalli et al. (2003). For the thermal component, we assumed a black body with temperature $kT = 0.7$ keV. The normalization of this component was then adjusted to match the observations at $E < 3$ keV.

In order to compute the possible contribution from heavily-obscured AGN to the stacked spectrum we assumed the observed X-ray spectrum of the nearby ULIRG IRAS19254-7245, as observed by Suzaku (Braitto et al. 2009). In addition to the starburst emission described above, the X-ray spectrum is described by an absorbed, Compton-thick, power-law with $\Gamma = 1.9$, $N_H = 10^{24}$ cm⁻², and a possible scattered component, characterized by a power-law with $\Gamma = 1.9$, no absorption, and 1% of the intensity of the direct emission. The resulting simulated spectral components and the comparison with the observed stacked spectrum for sources with the four samples defined above are shown in Fig. 2.

It is not possible to explain the observed stacked spectral shape using only a plausible starburst spectrum without invoking an AGN component, which dominates at $E > 5$ keV. The average intrinsic rest-frame 2-10 keV AGN luminosity needed to explain the observed spectrum, assuming that every source in the sample contains an AGN of the same luminosity, is 6×10^{42} erg s⁻¹ for sources with $L_{IR} > 10^{11} L_\odot$, 3×10^{42} erg s⁻¹ for sources with $L_{IR} > 5 \times 10^{10} L_\odot$, 5×10^{41} erg s⁻¹ in the sample with $5 \times 10^{10} L_\odot > L_{IR} > 10^{10} L_\odot$ and 7×10^{41} erg s⁻¹ for sources with $L_{IR} > 10^{10} L_\odot$. All of these are (intrinsically) very low-luminosity AGN; even if there is a range, it is extremely unlikely to include high-luminosity quasars like those discussed in previous stacking papers. An alternative possibility is that the extra emission at $E > 5$ keV is due entirely to the Fe $K\alpha$ line, provided the errors in the photometric redshifts in these samples are significantly larger than the values reported by Cardamone et al. (2010a). Regardless of the template assumed for the AGN emission, we obtain similar values for the average AGN luminosity in each sample.

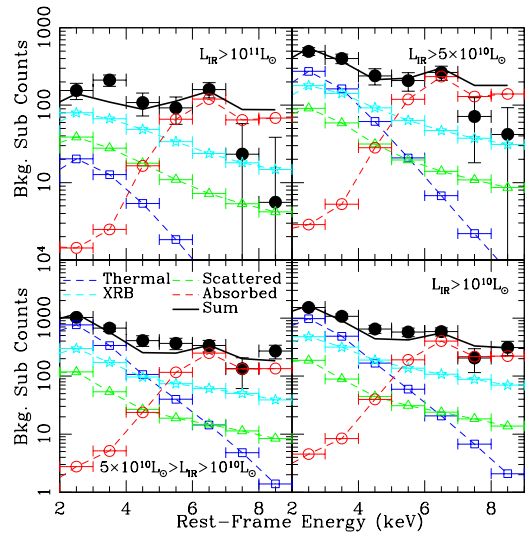


FIG. 2.— Stacked background-subtracted Chandra counts as a function of rest-frame energy, as in Fig. 1. *Black data points (filled circles)* show the stacked X-ray signal for sources binned by IR luminosity. The *cyan dashed lines (stars)* shows the simulated spectra for the HMXB population normalized using the Ranalli et al. (2003) relation between star-formation rate and X-ray luminosity. The *blue dashed lines (open squares)* show simulated thermal spectra corresponding to a black body with $kT = 0.7$ keV, required to explain the $E < 3$ keV emission. An absorbed AGN spectrum, given by a power-law with $\Gamma = 1.9$ and a fixed $N_H = 10^{24}$ cm⁻², is shown by the *red dashed lines (open circles)*. In addition, a scattered AGN component, characterized by a 1% reflection of the underlying unobscured power-law, is shown by the *green dashed lines (open triangles)*. The resulting summed spectrum (*black solid lines*) is in very good agreement with the observed counts. The strong detection in the stacked spectrum at $E > 5$ keV, in particular at the higher IR luminosities, confirms the presence of a significant number of heavily-obscured AGN in these samples.

The median hard X-ray luminosity for the Chandra sources with measured photometric redshifts in the catalog of Luo et al. (2008) is 4.1×10^{43} erg s⁻¹ for the sources in the $L_{IR} > 10^{11} L_\odot$ sample, 3.5×10^{43} erg s⁻¹ in the $L_{IR} > 5 \times 10^{10} L_\odot$ group, 5.7×10^{42} erg s⁻¹ for sources with $5 \times 10^{10} L_\odot > L_{IR} > 10^{10} L_\odot$ and 1.6×10^{43} erg s⁻¹ in the $L_{IR} > 10^{10} L_\odot$ sample. Hence, if the heavily-obscured AGN in our stacked samples have the same median intrinsic luminosity this would indicate that 15% (98 sources) of the 670 galaxies with $L_{IR} > 10^{11} L_\odot$ contain a heavily-obscured AGN. This fraction is $\sim 9\%$ (132 and 205 sources respectively) in the $L_{IR} > 5 \times 10^{10} L_\odot$ and $5 \times 10^{10} L_\odot > L_{IR} > 10^{10} L_\odot$ samples. For sources with $L_{IR} > 10^{10} L_\odot$ this fraction is $< 5\%$. The integrated intrinsic X-ray emission in the rest-frame 2-10 keV band due to the heavily-obscured AGN in this sample, obtained by multiplying the intrinsic X-ray luminosity by the number of sources and dividing by the studied area, is $\sim 4.6 \times 10^{46}$ erg cm⁻² s⁻¹ deg⁻². For comparison, the total emission from all the X-ray detected AGN in the CDF-S is 1.63×10^{47} erg cm⁻² s⁻¹ deg⁻². Hence, this extra AGN activity can account for $\sim 22\%$ of the total SMBH accretion. Adding this to the obscured SMBH growth in X-ray detected AGN (Luo et al. 2008), we confirm that most SMBH growth, $\sim 70\%$, is significantly obscured and missed by even the deepest X-ray surveys

⁷ Obtained from <http://cxc.harvard.edu/caldb/calibration/acis.html>

(Treister et al. 2004, 2010).

Performing a similar study on the 28 sources with $f_{24}/f_R > 1000$ and $R-K > 4.5$ that we previously excluded, we find a very hard X-ray spectrum, harder than that of the $L_{IR} > 10^{11} L_\odot$ sources. This spectrum is consistent with a population of luminous AGN with intrinsic rest-frame 2-10 keV luminosity $\sim 2 \times 10^{43}$ erg s $^{-1}$ and negligible contribution from the host galaxy, except at $E < 2$ keV where the thermal component is $\sim 30\%$ of the total emission. This result justifies our choice of removing these sources from our study (otherwise they would dominate the stacked signal), while at the same time it confirms the AGN nature of the vast majority of these sources, in contrast to the suggestion that the extra IR emission could be due to star-formation processes (Donley et al. 2008; Pope et al. 2008; Georgakakis et al. 2010). A similar result for these high-luminosity sources was found by Fiore (2010): In a sample of 99 mid-IR excess sources in the COSMOS field he found a strong stacked signal at $E \sim 6$ keV, which he interpreted as due to the Fe K α line, a clear signature of AGN emission and high obscuration (see discussion below).

3.1. Multiwavelength Properties

By design, none of the sources in our sample are individually detected in X-rays, nor do they satisfy the selection criteria of Fiore et al. (2008). However, it is interesting to investigate if they present other AGN signatures. For example, 237 out of the 1545 sources with $L_{IR} > 5 \times 10^{10} L_\odot$ in our sample (15%) are found inside the AGN IRAC color-color region defined by Stern et al. (2005). For comparison, in the sample of 2342 sources with $5 \times 10^{10} L_\odot > L_{IR} > 10^{10} L_\odot$ — in which from the stacked hard X-ray signal we determined a negligible AGN fraction — there are 327 galaxies (14%) in the Stern et al. (2005) region. This suggests that the IRAC color-color diagram cannot be used to identify heavily-obscured low-luminosity AGN, because the near-IR emission in these sources is dominated by the host galaxy (Cardamone et al. 2008). At longer wavelengths, 83 of the 1545 sources with $L_{IR} > 5 \times 10^{10} L_\odot$ were detected in the deep VLA observations of the CDF-S (Kellermann et al. 2008). In contrast, only 33 sources in the $5 \times 10^{10} L_\odot > L_{IR} > 10^{10} L_\odot$ sample were detected in these observations. Using the q_{24} ratio between 1.4 GHz and 24 μ m flux densities (e.g., Appleton et al. 2004), we find that in the $L_{IR} > 5 \times 10^{10} L_\odot$ sample, only 14 sources have $q_{24} < -0.23$ and can be considered “radio-loud” (Ibar et al. 2008), and in the $5 \times 10^{10} L_\odot > L_{IR} > 10^{10} L_\odot$ sample only 10 sources have $q_{24} < -0.23$. Hence, we conclude that the fraction of bona fide radio-loud sources is negligible and that in most cases the radio emission is produced by star-formation processes.

3.2. AGN Fraction Versus Stellar Mass

In order to investigate the fraction of heavily-obscured AGN as a function of other galaxy parameters, we performed X-ray stacking of samples sorted by stellar mass. Stellar masses were taken from Cardamone et al. (2010a), who performed spectral fitting to the extensive optical and near-IR spectro-photometry using FAST (Kriek et al. 2009) and the stellar templates of Maraston (2005) assuming the Kroupa (2001) initial mass function and solar metallicity. We further restricted our

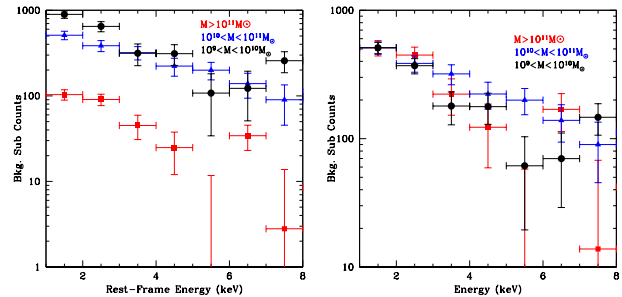


FIG. 3.— Stacked Chandra counts for galaxies binned as a function of their stellar mass. The *left panel* shows the spectra for the following bins: $M > 10^{11} M_\odot$ (red squares), $10^{10} < M < 10^{11} M_\odot$ (blue triangles) and $10^9 < M < 10^{10} M_\odot$ (black circles). *Right panel*: same but normalized at 1 keV. In the $M > 10^{11} M_\odot$ sample, the strong excess at $E=6-7$ keV, which we associate with the Fe K α line, is an indicator of AGN activity. Similarly, for the sources with $10^{10} < M < 10^{11} M_\odot$ there is a hard X-ray spectrum, also suggesting a significant AGN fraction. These preliminary results indicate that these heavily-obscured moderate-luminosity AGN are predominantly present in the most massive galaxies.

sample to sources with $z < 1.2$, for which photometric redshifts and stellar masses are very well determined ($\Delta z/(1+z) = 0.007$). We then divided the sample into three mass bins: $M > 10^{11} M_\odot$, $10^{11} > M (M_\odot) > 10^{10}$ and $10^{10} > M (M_\odot) > 10^9$. The resulting stacked X-ray spectra are shown in Fig. 3.

For sources with $M > 10^{11} M_\odot$, there is a significant excess at 6-7 keV, above a spectrum that otherwise declines with increasing energy. This might be due to the presence of the Fe K α line, a clear indicator of AGN activity. Contrary to the case of stacking as a function of IR luminosity (Fig. 2), here we do not find evidence for an absorbed power-law — the 6-7 keV feature is simply too sharply peaked. Possibly the restriction to $z < 1.2$ for the mass-binned stacking, where photometric redshifts are most accurate, reveals an emission line that is broadened by less accurate photometric redshifts in the full sample. That is, the feature in the L_{IR} -binned stack that we interpreted as a heavily absorbed power law may instead be an Fe K α line broadened artificially by bad photometric redshifts. In the $10^{11} > M (M_\odot) > 10^{10}$ sample we found a significant hardening of the X-ray spectrum (Fig. 3), suggesting the presence of a significant fraction of AGN. In contrast, only a soft spectrum, consistent with star-formation emission, can be seen for sources with $10^{10} > M (M_\odot) > 10^9$. Taken together, these results indicate that AGN are predominantly present in the most massive galaxies, in agreement with the conclusions of Cardamone et al. (2010b) and others. This will be elaborated in a paper currently in preparation.

3.3. Space Density of Heavily-Obscured AGN

The fraction of Compton-thick AGN in the local Universe is still heavily debated. Treister et al. (2009a) reported a fraction of $\sim 8\%$ in a flux-limited sample of sources detected in the Swift/BAT all-sky (Tueller et al. 2008) and International Gamma-Ray Astrophysics Laboratory (INTEGRAL; Krivonos et al. 2007) surveys. From an INTEGRAL volume-limited survey at $z < 0.015$, Malizia et al. (2009) found a higher fraction of 24%, sug-

gesting that even surveys at $E > 10$ keV are potentially biased against the detection of Compton-thick AGN. The fraction of moderate-luminosity Compton-thick sources in our sample of sources with $L_{IR} > 5 \times 10^{10} L_{\odot}$, relative to all AGN in the CDF-S, is $\sim 25\%$ (132/525), assuming that Compton-thick and Compton-thin AGN have similar median intrinsic luminosities. This indicates that there is no major evolution in the number of moderate-luminosity heavily-obscured AGN from $z=0$ to 2. In contrast, at higher luminosities, Treister et al. (2010) reported that the ratio of obscured to unobscured quasars increased from ~ 1 at $z=0$ to $\sim 2-3$ at $z \simeq 2$. Hence, although all these estimates are still uncertain, it appears that the evolution of Compton-thick AGN depends strongly on their luminosity. We further speculate that this is indication that the triggering of low-luminosity AGN is not related to the major merger of gas-rich galaxies as found by Treister et al. (2010) for high-luminosity

quasars or that the time delay between galaxy interactions and black hole growth is long (Schawinski et al. 2010b).

We thank the referee, Fabrizio Fiore, for very useful and constructive comments. Support for the work of ET and KS was provided by the National Aeronautics and Space Administration through Chandra/Einstein Postdoctoral Fellowship Award Numbers PF8-90055 and PF9-00069 respectively issued by the Chandra X-ray Observatory Center, which is operated by the Smithsonian Astrophysical Observatory for and on behalf of the National Aeronautics Space Administration under contract NAS8-03060. CMU and CC acknowledge support from NSF grants AST-0407295, AST-0449678, AST-0807570 and Yale University.

REFERENCES

- Appleton, P. N. et al. 2004, *ApJS*, 154, 147
 Arnaud, K. A. 1996, in *ASP Conf. Ser. 101: Astronomical Data Analysis Software and Systems V*, ed. G. H. Jacoby & J. Barnes, 17–+
 Bauer, F. E., Yan, L., Sajina, A., & Alexander, D. M. 2010, *ApJ*, 710, 212
 Braito, V., Della Ceca, R., Piconcelli, E., Severgnini, P., Bassani, L., Cappi, M., Franceschini, A., Iwasawa, K., Malaguti, G., Marziani, P., Palumbo, G. G. C., Persic, M., Risaliti, G., & Salvati, M. 2004, *A&A*, 420, 79
 Braito, V., Franceschini, A., Della Ceca, R., Severgnini, P., Bassani, L., Cappi, M., Malaguti, G., Palumbo, G. G. C., Persic, M., Risaliti, G., & Salvati, M. 2003, *A&A*, 398, 107
 Braito, V., Reeves, J. N., Della Ceca, R., Ptak, A., Risaliti, G., & Yaqoob, T. 2009, *A&A*, 504, 53
 Brandt, W. N., Alexander, D. M., Hornschemeier, A. E., Garmire, G. P., Schneider, D. P., Barger, A. J., Bauer, F. E., Broos, P. S., Cowie, L. L., Townsley, L. K., Burrows, D. N., Chartas, G., Feigelson, E. D., Griffiths, R. E., Nousek, J. A., & Sargent, W. L. W. 2001, *AJ*, 122, 2810
 Cardamone, C. N., Urry, C. M., Damen, M., van Dokkum, P., Treister, E., Labbé, I., Virani, S. N., Lira, P., & Gawiser, E. 2008, *ApJ*, 680, 130
 Cardamone, C. N. et al. 2010a, *ApJS*, 189, 270
 Cardamone, C. N., Urry, C. M., Schawinski, K., Treister, E., Brammer, G., & Gawiser, E. 2010b, *ApJ* in press, arXiv:1008.2971
 Daddi, E. et al. 2007, *ApJ*, 670, 173
 Donley, J. L., Rieke, G. H., Pérez-González, P. G., & Barro, G. 2008, *ApJ*, 687, 111
 Fabian, A. C. & Iwasawa, K. 1999, *MNRAS*, 303, L34
 Fiore, F. 2010, in *American Institute of Physics Conference Series*, Vol. 1248, American Institute of Physics Conference Series, ed. A. Comastri, L. Angelini, & M. Cappi, 373–380
 Fiore, F. et al. 2008, *ApJ*, 672, 94
 —. 2009, *ApJ*, 693, 447
 Fruscione, A. et al. 2006, in *Presented at the Society of Photo-Optical Instrumentation Engineers (SPIE) Conference*, Vol. 6270, Society of Photo-Optical Instrumentation Engineers (SPIE) Conference Series
 Georgakakis, A., Rowan-Robinson, M., Nandra, K., Digby-North, J., Pérez-González, P. G., & Barro, G. 2010, *MNRAS*, 406, 420
 Hinshaw, G. et al. 2009, *ApJS*, 180, 225
 Ibar, E., Cirasuolo, M., Ivison, R., Best, P., Smail, I., Biggs, A., Simpson, C., Dunlop, J., Almaini, O., McLure, R., Foucaud, S., & Rawlings, S. 2008, *MNRAS*, 386, 953
 Iwasawa, K., Sanders, D. B., Evans, A. S., Mazzarella, J. M., Armus, L., & Surace, J. A. 2009, *ApJ*, 695, L103
 Kartaltepe, J. S. et al. 2010, *ApJ*, 709, 572
 Kellermann, K. I., Fomalont, E. B., Mainieri, V., Padovani, P., Rosati, P., Shaver, P., Tozzi, P., & Miller, N. 2008, *ApJS*, 179, 71
 Kriek, M., van Dokkum, P. G., Labbé, I., Franx, M., Illingworth, G. D., Marchesini, D., & Quadri, R. F. 2009, *ApJ*, 700, 221
 Krivonos, R., Revnivtsev, M., Lutovinov, A., Sazonov, S., Churazov, E., & Sunyaev, R. 2007, *A&A*, 475, 775
 Kroupa, P. 2001, *MNRAS*, 322, 231
 Lehmer, B. D. et al. 2005, *ApJS*, 161, 21
 Luo, B. et al. 2008, *ApJS*, 179, 19
 Lutovinov, A., Revnivtsev, M., Gilfanov, M., Shtykovski, P., Molkov, S., & Sunyaev, R. 2005, *A&A*, 444, 821
 Malizia, A., Stephen, J. B., Bassani, L., Bird, A. J., Panessa, F., & Ubertini, P. 2009, *MNRAS*, 399, 944
 Maraston, C. 2005, *MNRAS*, 362, 799
 Martínez-Sansigre, A., Rawlings, S., Lacy, M., Fadda, D., Jarvis, M. J., Marleau, F. R., Simpson, C., & Willott, C. J. 2006, *MNRAS*, 370, 1479
 Matt, G., Perola, G. C., & Piro, L. 1991, *A&A*, 247, 25
 Persic, M. & Rephaeli, Y. 2002, *A&A*, 382, 843
 Pope, A. et al. 2008, *ApJ*, 689, 127
 Ranalli, P., Comastri, A., & Setti, G. 2003, *A&A*, 399, 39
 Risaliti, G., Maiolino, R., & Salvati, M. 1999, *ApJ*, 522, 157
 Rubin, K. H. R., van Dokkum, P. G., Coppi, P., Johnson, O., Förster Schreiber, N. M., Franx, M., & van der Werf, P. 2004, *ApJ*, 613, L5
 Schawinski, K. et al. 2010a, *ApJ*, 711, 284
 Schawinski, K., Dowlin, N., Thomas, D., Urry, C. M., & Edmondson, E. 2010b, *ApJ*, 714, L108
 Stern, D., Eisenhardt, P., Gorjian, V., Kochanek, C. S., Caldwell, N., Eisenstein, D., Brodwin, M., Brown, M. J. I., Cool, R., Dey, A., Green, P., Jannuzi, B. T., Murray, S. S., Pahre, M. A., & Willner, S. P. 2005, *ApJ*, 631, 163
 Takeuchi, T. T., Buat, V., Iglesias-Páramo, J., Boselli, A., & Burgarella, D. 2005, *A&A*, 432, 423
 Teng, S. H., Veilleux, S., Anabuki, N., Dermer, C. D., Gallo, L. C., Nakagawa, T., Reynolds, C. S., Sanders, D. B., Terashima, Y., & Wilson, A. S. 2009, *ApJ*, 691, 261
 Teng, S. H., Wilson, A. S., Veilleux, S., Young, A. J., Sanders, D. B., & Nagar, N. M. 2005, *ApJ*, 633, 664
 Treister, E., Natarajan, P., Sanders, D. B., Urry, C. M., Schawinski, K., & Kartaltepe, J. 2010, *Science*, 328, 600
 Treister, E., Urry, C. M., & Virani, S. 2009a, *ApJ*, 696, 110
 Treister, E. et al. 2004, *ApJ*, 616, 123
 —. 2009b, *ApJ*, 706, 535
 Tueller, J., Mushotzky, R. F., Barthelmy, S., Cannizzo, J. K., Gehrels, N., Markwardt, C. B., Skinner, G. K., & Winter, L. M. 2008, *ApJ*, 681, 113
 Virani, S. N., Treister, E., Urry, C. M., & Gawiser, E. 2006, *AJ*, 131, 2373